Active Droplet Oscillation Excited by Optimized Waveform

Experiments reveal the effects of waveform parameters on the excited droplet oscillation, plus the optimal range of current waveform parameters is determined

BY J. XIAO, G. J. ZHANG, S. J. CHEN, L. WU, AND Y. M. ZHANG

ABSTRACT

The active droplet oscillation method is an approach previously proposed to detach the droplet at currents below the transition current. In this method, a droplet oscillation is first excited by intentionally switching the current from the peak to base level; the downward momentum of the oscillating droplet is then utilized to enhance the droplet detachment such that the droplet can be detached at reduced peak currents lower than the transition current. In the present work, this method is systematically studied to initiate stronger oscillations with lower average currents. To this end, the current waveform is modified by differentiating the exciting current from the growing current. This differentiation enables the growing current (heat input) be reduced without affecting the oscillation excitation. The current waveform is then further modified by adding a base period before the exciting pulse to maximize the oscillation, resulting in an optimized waveform. A series of experiments has been conducted to correlate the droplet oscillation to the parameters in the optimized waveform. The optimal ranges for the waveform parameters are experimentally determined. The active droplet oscillation method is improved at a fundamental level, and its mechanism is also better understood.

Introduction

Gas metal arc welding (GMAW) is currently the most widely used arc welding method in the manufacturing industry due to its high productivity by using a consumable wire and its good compatibility to automatic welding. The formation and detachment of the metal droplet is generally referred to as the metal transfer process, which plays a critical role in determining the arc stability and welding quality; therefore, effective control of the metal transfer helps improve the GMAW process for better stability and weld quality (Refs. 1, 2).

The metal transfer is typically classified into three modes — short circuiting transfer, globular transfer, and spray transfer. Spray transfer can be further classified into drop (projected) spray and streaming spray (Ref. 3). With relatively low welding currents, the transfer mode is expected to be short circuiting or globular transfer, which both often produce unstable arc and significant spatters unless appropriate controls such as surface tension transfer (STT) and cold metal transfer (CMT) (Refs. 4–6) are applied. When the welding current increases to be higher than the transition current (Ref. 3), the transfer mode changes into the spray transfer in which the droplet is detached at a diameter similar to that of the wire. A further increase in the current would result in the streaming spray where the impact from high-speed small particles on the weld pool may produce undesirable finger-shaped penetration (Refs. 7–10).

While drop spray, which is generally associated with good stability and low spatter, is often the preferred transfer mode, its required amperage — higher than the transition current, resulting in increased heat input, metal vapors, and arc pressures — may not always be preferred. Welding researchers are motivated to develop methods that use currents lower than the transition currents to produce drop spray transfer. According to the dynamic force model balance (DFMB) theory on metal transfer (Ref. 11), the electromagnetic force determined by the welding current is the primary detaching force, and the gravitational force, plasma gas drag force, and momentum force also contribute to droplet detachment. The major retaining force that resists the droplet detachment is the surface tension. When the detaching force is greater than the retaining force, the droplet is detached from the wire tip. Based on this theory, the approaches developed to achieve spray transfer have focused on changing the forces on the droplet using electrical and mechanical ways (Refs. 12–17).

Pulsed gas metal arc welding (GMAW-P) is a widely used electrical way to produce the desired drop spray transfer at a wide range of average current (Refs. 14, 18). In GMAW-P, the desired one droplet per pulse (ODPP) transfer is achieved by selecting an appropriate combination of the duration and amplitude of the peak current. Basically, the amplitude of the peak current still needs to be higher than the transition current to avoid one droplet multiple pulses (ODMP) while its duration needs to be appropriately short to avoid multiple droplets per pulse (Refs. 19, 20) and appropriately long to ensure the detachment for ODMP. Achieving the desired droplet ODPP transfer using GMAW-P through optimizing parameters may not be robust enough while a peak

J. XIAO is with the National Key Laboratory of Advanced Welding and Joining, Harbin Institute of Technology, China, and the Institute for Sustainable Manufacturing, University of Kentucky, Lexington, Ky. G. J. ZHANG and L. WU are with the National Key Laboratory of Advanced Welding and Joining, Harbin Institute of Technology, China. S. J. CHEN is with the Welding Research Institute, Beijing University of Technology, China. Y. M. ZHANG (yuming.zhang@uky.edu) *is with the Institute for Sustainable Manufacturing and Department of Electrical and Computer Engineering, University of Kentucky, Lexington, Ky.*

KEYWORDS

Droplet
Oscillation
Waveform
Metal Transfer
Transition Current
Spray Transfer

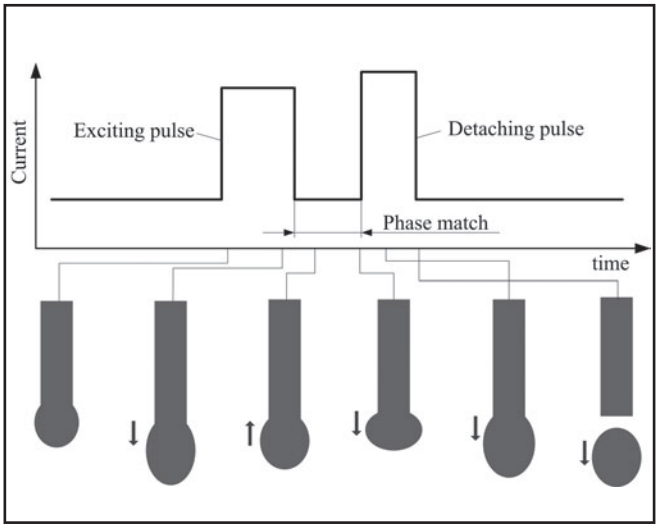

Fig. 1 — Active metal transfer by monitoring the excited droplet oscillation.

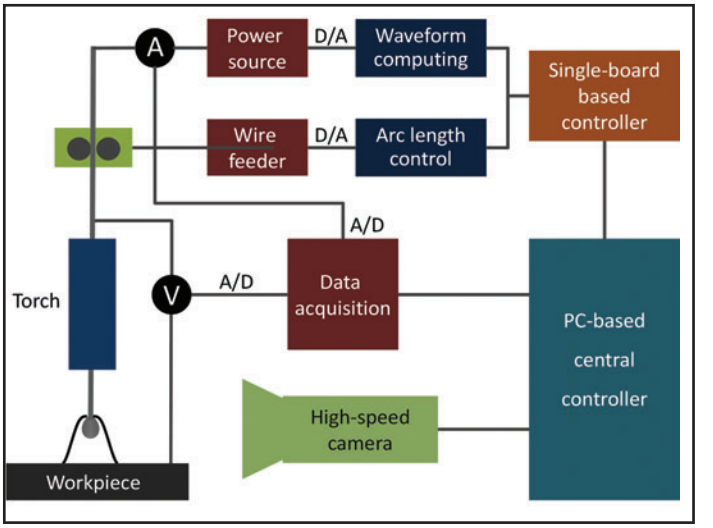

Fig. 2 — Schematic of the experimental system.

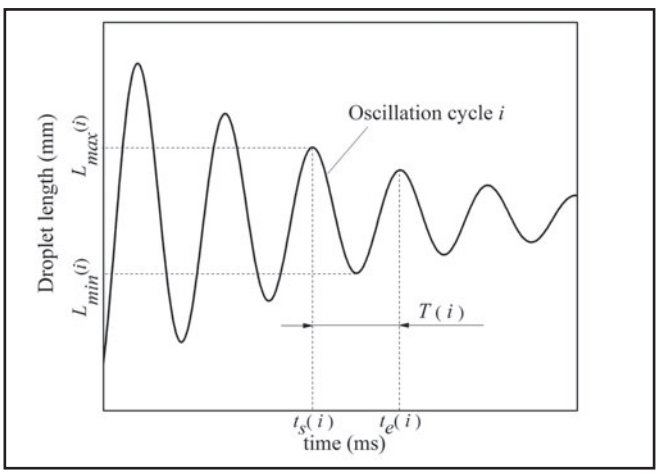

Fig. 3 — Sketch of the droplet oscillation.

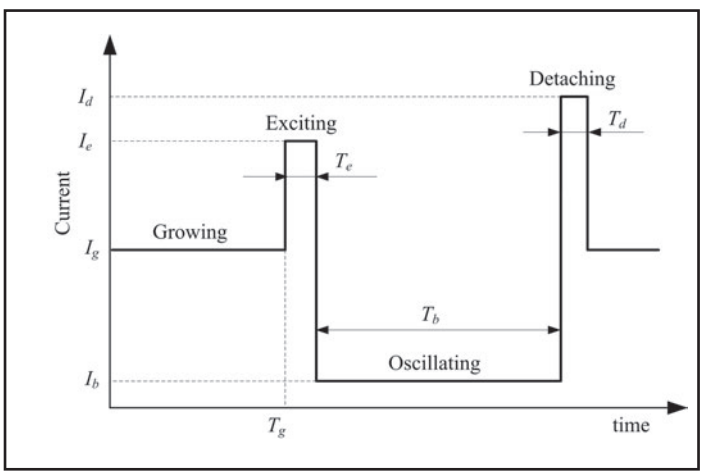

Fig. 4 — Simple current waveform for the separation-based modification.

current higher than the transition current is still needed.

A method has been proposed to achieve a robust control for repeatable and controllable metal transfer in GMAW-P with reduced peak current amperage, referred to as active control of metal transfer, by using an excited droplet oscillation (Refs. 21–23). The droplet is actively oscillated to generate a downward momentum that will significantly enhance the droplet detachment. As shown in Fig. 1, during the exciting pulse, the droplet grows gradually at the same amperage as the exciting current and is dragged into an elongated shape with initial amplitude in the weld pool direction by the electromagnetic force. Then the current is switched from the exciting level to the base level, so the electromagnetic force decreases, and the droplet springs back to the wire tip and starts oscillating due to the surface tension.

When the downward motion of the droplet is first detected, the current is increased to the detaching level. With the assistance of the downward momentum, the droplet detachment is ensured with a detaching current lower than the spray transition current, which is essential in conventional GMAW-P. The synchronization of the detaching current and downward momentum of the droplet is referred to as phase match. In Ref. 24, this method has been modified to suit for metal transfer control for titanium by applying appropriate current levels, but the current waveform is unchanged.

In the dynamic force balance model (DFBM), a mass-spring system is used to model the droplet oscillation (Ref. 11). The dynamic droplet motion is described as a second-order system varying with time as follows:

$$m(t)\ddot{x} + c(t)\dot{x} + k(t)x = F(t)$$

where x represents the mass center displacement in the axial direction, F is the axial force exerted on the droplet, and m, c, and k are the mass, damping coefficient, and spring constant of the droplet, respectively. The surface tension acts as a spring force. In literature (Ref. 11), the droplet oscillation under continuous current is numerically analyzed. The droplet oscillation under the pulsed current condition is studied in literature (Ref. 25). The numerical computation results in Refs. 11 and 25 both demonstrate that the droplet oscillation frequency is mainly determined by the droplet mass.

With respect to the active droplet oscillation, the previous research focused on introducing its novel principle. However, the associated oscillation was not fully studied. In particular, the exciting pulse current was fixed at a high level (220 A for a 1.2-mm-diameter wire) to ensure that the droplet could be elongated and oscil-

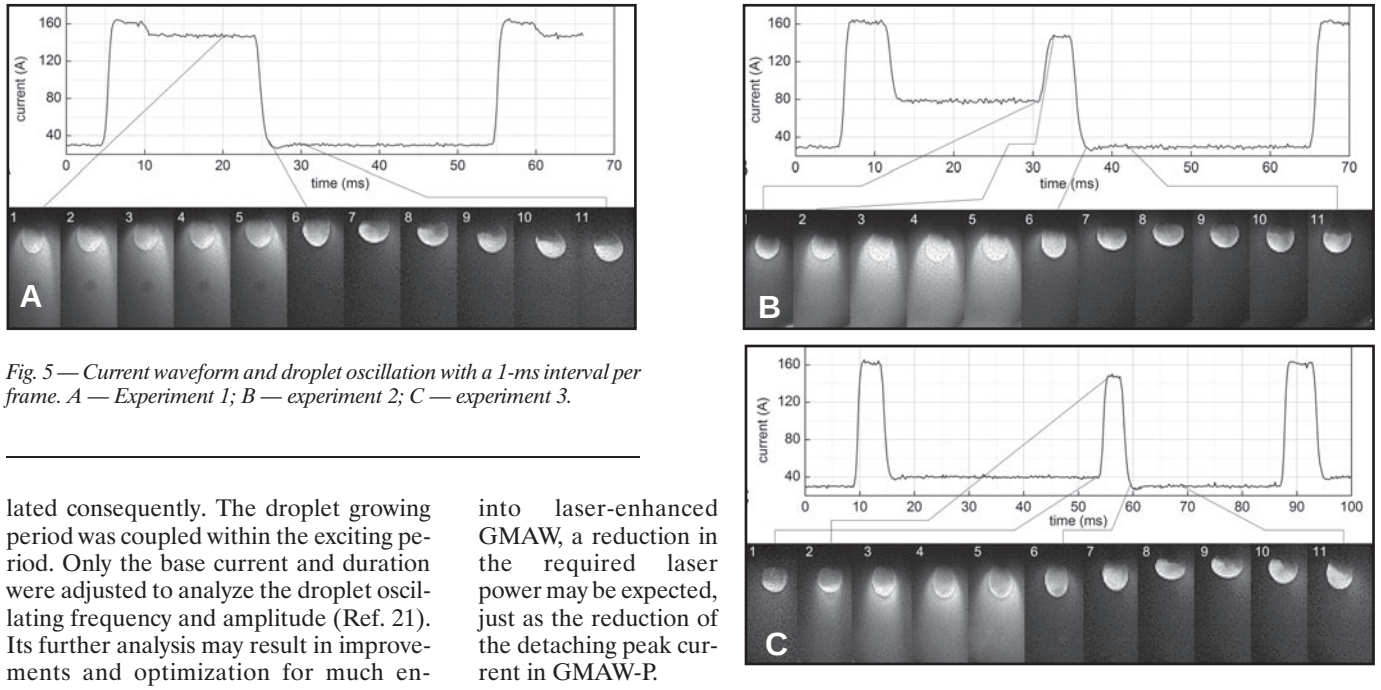

Fig. 5 — Current waveform and droplet oscillation with a 1-ms interval per frame. A — Experiment 1; B — experiment 2; C — experiment 3.

lated consequently. The droplet growing period was coupled within the exciting period. Only the base current and duration were adjusted to analyze the droplet oscillating frequency and amplitude (Ref. 21). Its further analysis may result in improvements and optimization for much enhanced metal transfer control abilities.

In particular, the excited droplet oscillation is a damping process. The initial displacement of the droplet that determines the initial oscillating energy increases with the exciting peak current. However, in the original active oscillation method, this exciting peak current is the same with the current that grows the droplet. If a lower and adjustable growing current is used to form the droplet as determined by the application, and then a shorter exciting pulse is applied to excite the droplet oscillation, the growing and exciting processes can be separately controlled. The metal transfer control achieved by the active oscillation method may be improved.

Active droplet oscillation can be considered as an electrical control strategy for metal transfer. This active control technology can be applied not only in GMAW-P as a modified GMAW-P process, but also can be coupled with other control methods to improve the original process such as laser-enhanced GMAW, a method recently developed to actively control the metal transfer at given arc variables (Ref. 26). In such a process, a laser beam irradiating on the droplet is applied to vaporize the droplet partially. A recoil force is generated as an additional detaching force to enhance droplet detachment. As a result, short circuiting transfer under a range of welding currents becomes controlled globular transfer or even drop spray transfer. Therefore, the metal transfer and heat input, respectively, can be freely controlled. Welding spatter is also reduced significantly, and the arc stability is improved (Refs. 27, 28). However, the requirement on the laser power restricts its application in industry. If the active droplet oscillation technology is combined into laser-enhanced GMAW, a reduction in the required laser power may be expected, just as the reduction of the detaching peak current in GMAW-P.

In this paper, the active droplet oscillation process is further analyzed and optimized. A modified current waveform is proposed in which the droplet growing and oscillation exciting are decoupled and become separately controllable. The growing current can be set no longer as high as the exciting peak current. The average welding current decreases. On the other hand, the exciting peak duration can be set very narrow, which is expected to generate enough electromagnetic force to elongate the droplet prominently but not melt the wire significantly. Based on the observation and analysis of the preliminary results, the

Table 1 — Definitions of Variables in Oscillation Description

Symbol	Definition
L_{int}	Initial droplet length measured at the end of the growing period
$A(i)$	Droplet oscillation amplitude of cycle i: $A(i) = L_{max}(i) - L_{min}(i)$
$T(i)$	Measured droplet oscillation period of cycle i: $T(i) = t_s(i) - t_e(i)$
A_{int}	Initial amplitude of the whole droplet oscillation duration: $A_{int} = L_{max}(0) - L_{int}$
A_{avg}	Average oscillation amplitude of N droplet oscillating cycles: $A_{avg} = \frac{1}{N}\sum_{i=0}^{N} A(i)$
T_{avg}	Average droplet oscillation period under certain waveform parameters: $T_{avg} = \frac{1}{N}\sum_{i=0}^{N} T(i)$

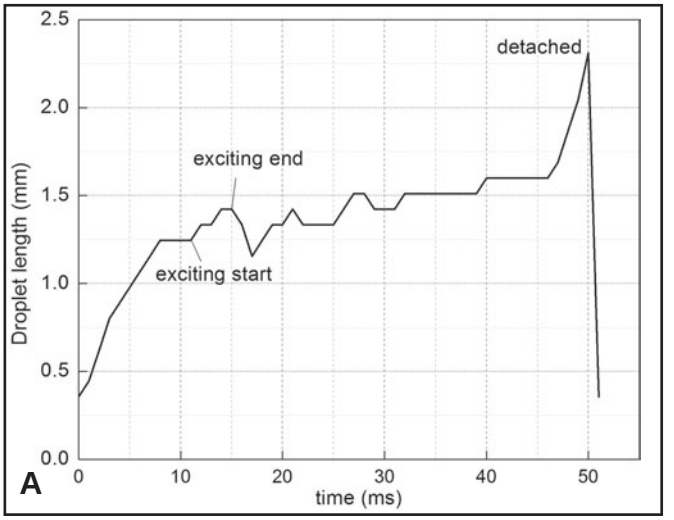

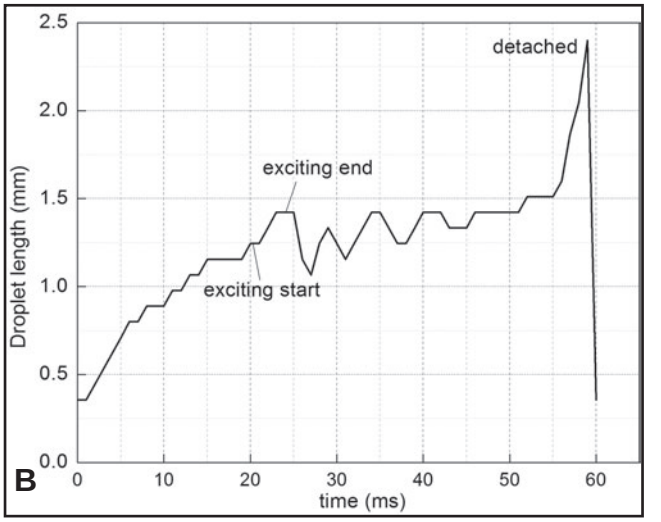

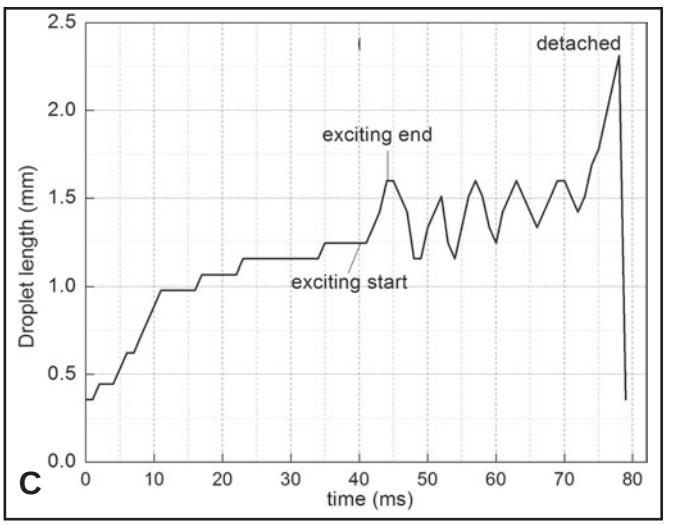

Fig. 6 — Dynamic curves of the droplet oscillation. A — Experiment 1; B — experiment 2; C — experiment 3.

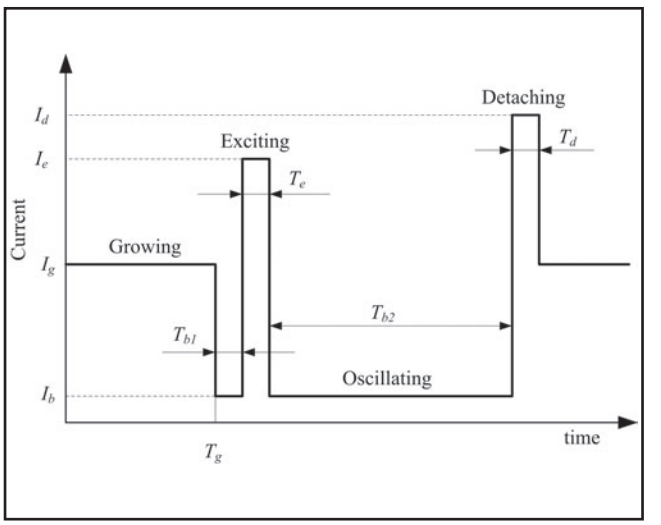

Fig. 7 — Optimized welding current waveform.

Table 2 — Growing Parameters in Experiments 1–3

No.	I_g (A)	T_g (ms)	Waveform
1	150	11	Original
2	80	20	Modified
3	40	40	Modified

Table 3 — Growing Parameters in Experiments 4, 5

No.	I_g (A)	T_g (ms)	Waveform
4	80	20	Optimized
5	150	11	Optimized

current waveform is further optimized to maximize the droplet oscillation energy despite the actual growing current level. The key factors that characterize the dynamic droplet oscillation, such as the amplitude, frequency, and rate of decay under different exciting parameters, are calculated to measure the droplet oscillation magnitude. By selecting an optimal combination of the exciting parameters, a much stronger droplet oscillation with significantly lower heat input are achieved. In this sense, the study improves the active oscillation method and furthers the understanding on the dynamic droplet oscillation behavior and mechanism.

Experimental System and Approach

Experimental Setup

The experimental setup is shown in Fig. 2. An inverter power source was used to conduct the welding experiments. It can be used for either constant current (CC) or constant voltage (CV) mode. In this work, the CC mode was selected to achieve the desired welding current waveform. The arc length was controlled to be stable by adjusting the wire feeding speed based on arc voltage feedback. The power supply and wire feeder can both be controlled by analog input signals. A single-board computer-based controller was established to compute the output waveform of the welding current and wire feed speed. A data-acquisition set was established to record the actual welding current and arc voltage waveform during the welding experiments, and an Olympus iSpeed-2 high-speed camera was used to observe and record the droplet oscillation. The data-acquisition board and high-speed camera both can be triggered to work by a 5-V TTL signal such that recording the arc variables and metal transfer is synchronized; therefore, the arc voltage signal can be further processed to analyze the droplet oscillation process. To view the highly dynamic characteristics of the droplet oscillation, the recording fre-

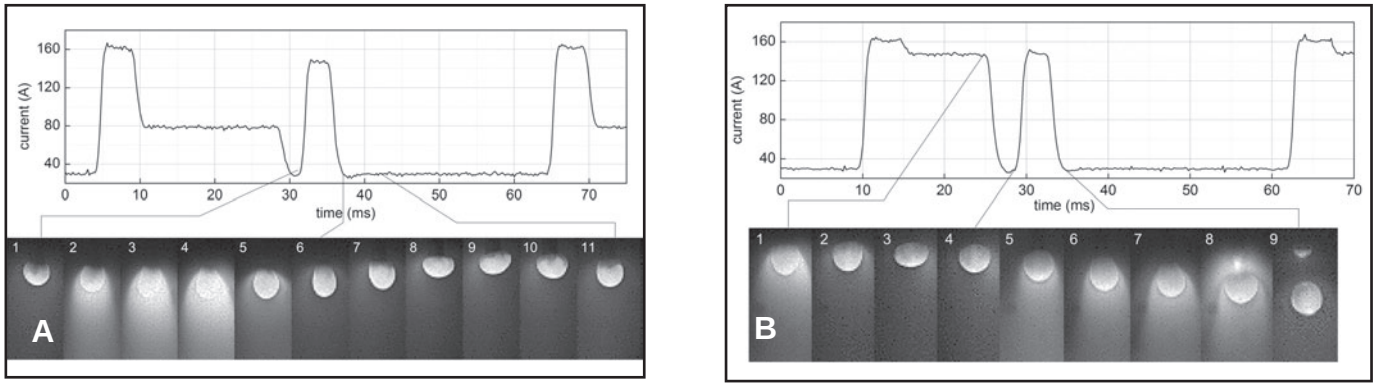

Fig. 8 — Droplet oscillation using the optimized current waveform with a 1-ms interval per frame. A — Experiment 4; B — experiment 5.

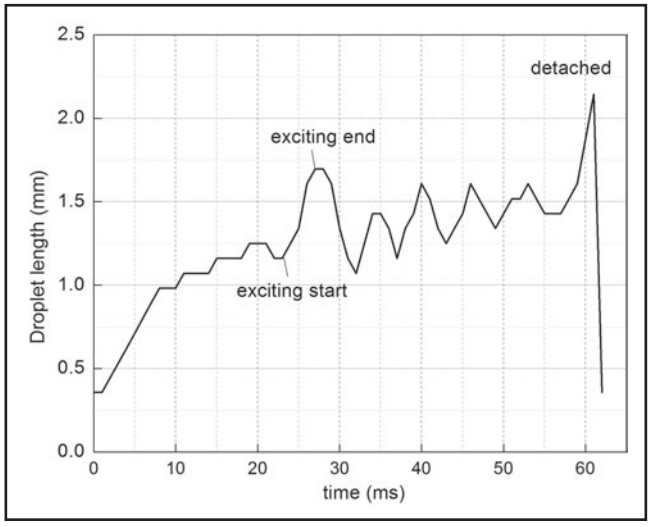

Fig. 9 — Dynamic curve of the droplet oscillation in experiment 4.

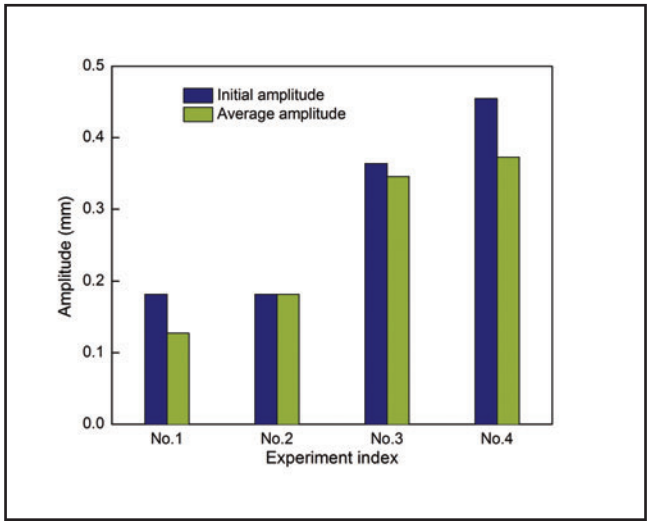

Fig. 10 — Droplet oscillation amplitudes measured from experiments 1–4.

quency was set at 5000 hz.

All the welding experiments were conducted as bead-on-plate welding with a travel speed of 3 mm/s; the base metal was mild steel; the wire was ER70S-6 with 0.8 mm diameter; and the distance from the contact tip to workpiece was set at 12 mm.

Experimental Study Steps

As mentioned earlier, the major modification introduced from this study is that the droplet growing and exciting are intentionally separated as two actions. That is, a lower growing current with a specified duration is applied to form the droplet. When the droplet reaches the desired size, the welding current is increased to the exciting peak level. This peak current is maintained for several milliseconds. During this exciting peak period, the droplet is elongated by the increased electromagnetic force. Due to this elongation, the droplet springs back to start oscillating when the current is switched to the base level. As can be seen, this modification involves a number of parameters that characterize the current waveform and may affect the effectiveness of the proposed modification. To optimize the modification, the experimental studies will follow pursuing three steps.

Feasibility Verification. The experiments in this step will be designed and used as examples to verify that the modification characterized by the separation of the exciting current from the growing current can help increase the initial energy of the oscillation. The average droplet diameter will be controlled to be slightly larger than the wire diameter to avoid the effect from the droplet mass.

Waveform Optimization. The separation of the exciting current from the growing current provides a modification to increase the oscillation. However, the separation method (current waveform) used above for the feasibility verification is a relatively simple one. To further take advantage of the separation, the effect of the separation is maximized by reducing the current from the growing current to the possible minimal level allowed, i.e., the base current, before the exciting pulse is applied. The waveform is further modified to maximize the oscillation.

Parameter Optimization. While the optimized waveform provides a type of current waveform that can further increase the oscillation using the separation principle, there are still parameters depicting the actual waveform and that can be optimized to maximize the oscillation. In this step, experiments are designed/conducted and the experimental data are analyzed to optimize these parameters.

Analysis Approach

High-speed droplet image sequences and actual arc variable waveforms are synchronously recorded by using the same trigger signal to analyze the oscillation. For quantitative analysis of the oscillation, the vertical coordinates of the droplet top and bottom are measured in pixels (11.25 pixels = 1 mm) from the recorded images. The droplet length can be calculated to describe the droplet oscillation behavior. The fluctuation of the measured droplet

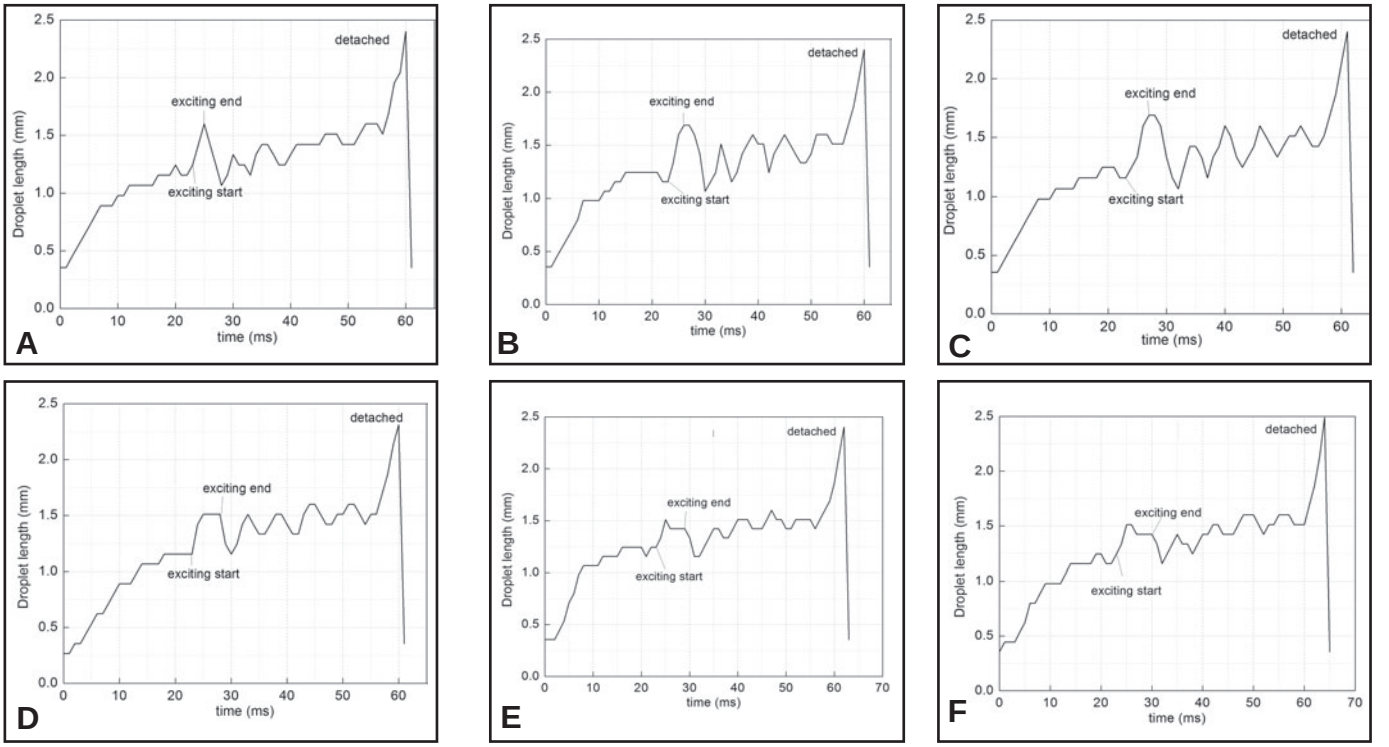

Fig. 11 — Droplet oscillation with different exciting peak durations. A — T_e = 2 ms; B — T_e = 3 ms; C — T_e = 4 ms; D — T_e = 5 ms; E — T_e = 6 ms; F — T_e = 7 ms.

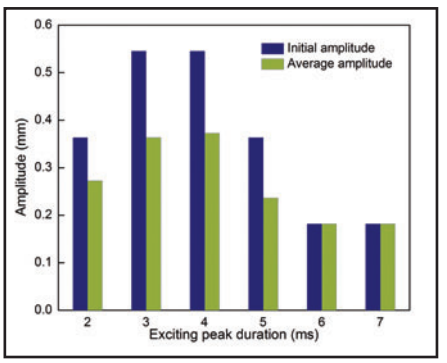

Fig. 12 — Droplet oscillation energy with different exciting peak durations.

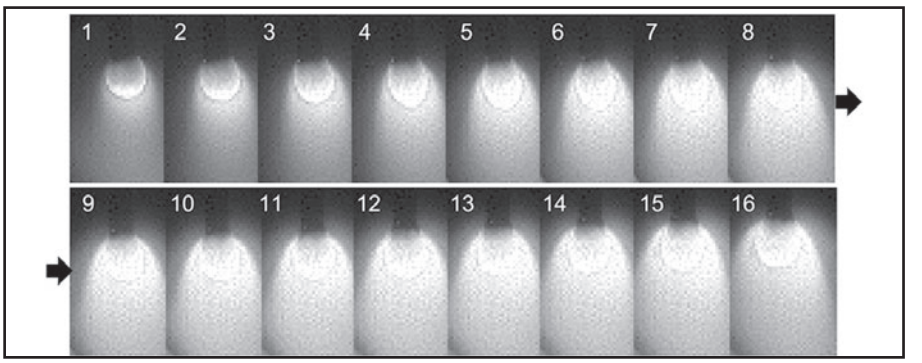

Fig. 13 — Droplet motion during the exciting period for experiment 11 with a 0.4-ms interval per frame.

length curve gives the droplet oscillation magnitude. However, in previous work (Ref. 21), only the coordinates of the droplet bottom position were measured to describe the oscillation. The top and bottom coordinates of the droplet can apparently be used to better describe and analyze the oscillation.

A standard damping oscillation is used to model the droplet oscillation in this study as shown in Fig. 3. The parameters in this model are self defined in Fig. 3 and explained in Table 1. In Table 1, N denotes the total oscillation cycles the droplet experiences from the end of the exciting pulse to the application of the detaching pulse.

In particular, at the end of the exciting pulse, the droplet oscillation starts. The initial amplitude A_{int} is used to represent the initial droplet oscillation energy for a given mass droplet. Because of possible errors in image measurement, the average amplitude of the droplet oscillation A_{avg} is defined to better quantify the droplet oscillation energy during the whole oscillating period. What should be pointed out is that each oscillating cycle is not isochronous because the droplet mass is still slowly increasing during the oscillation. Therefore, the droplet oscillation period and frequency cited in this paper are actually the average period and frequency. Also, in this paper, the oscillation of the droplet is quantitatively analyzed using the model and parameters together with high-speed images.

Simple Current Waveform for Separation

The effectiveness of separation as a modification to the active oscillation method is first verified using a simple current waveform as shown in Fig. 4. In this case, the whole metal transfer cycle is divided into four periods as follows: growing, exciting, oscillating, and detaching. The droplet grows gradually during the growing period at a relatively low current I_g. The initial droplet length L_{int} is controlled by adjusting the growing duration T_g. Then the current is increased to the exciting peak level I_e. The exciting peak duration T_e is expected to be as short as several milliseconds. The difference between the exciting peak current and growing current is defined as the exciting rising level I_R: $I_e - I_g$. Then the current is reduced to the exciting base level I_b, and this step-down level is defined as the exciting falling level I_F: $I_e - I_b$. The base duration T_b is set to be long enough to provide adequate

time for the droplet to oscillate. At the end of the base duration, the detaching current I_d is applied to guarantee the droplet detachment. Hence, the whole growing, exciting, oscillating, and detaching periods are periodically repeatable and controllable.

Experiments 1–3 were conducted to examine the droplet oscillation under the simple waveform modification. The growing parameters of the current waveform used in these three experiments are listed in Table 2. The growing period T_g has been intentionally changed with the growing current I_g to control the droplet diameter to be slightly greater than that of the wire. The droplet mass in these three experiments were controlled approximately the same such that the effect of the droplet mass on the oscillation can be excluded in the verification experiments.

The remaining waveform parameters in these experiments are fixed to be the same: I_e = 150 A, T_e = 4 ms; I_b = 30 A, T_b = 30 ms; and I_d = 165 A, T_d = 5 ms. It is apparent the oscillation in experiment 1, where the growing current equals the exciting current, is actually the oscillation excited using the original method. Its comparison with those in experiments 2 and 3 will be used to verify the effectiveness of the separation-based modification.

In particular, the exciting peak current I_e was set at 150 A based on that the actual transition current was experimentally measured to be 165 A under the aforementioned welding condition (wire diameter, shielding gas, etc.). The exciting peak duration T_e was 4 ms. The growing currents I_g were set at 150, 80, and 40 A for experiments 1–3, respectively. The growing durations T_g were correspondingly set at 11, 20, and 40 ms to keep the initial droplet size approximately even in the three experiments.

The average current in experiments 1–3 — 79.5, 66.5, and 49.7 A, respectively — can be easily calculated. It is quite clear that the heat input can be effectively reduced by using the modified current waveform. The droplet oscillations in these three experiments were analyzed from the obtained image sequences. A typical cycle of measured current waveforms and images of droplet oscillation are shown in Fig. 5A–C in which the time interval for each frame is 1 ms. Due to the rapid damping of the droplet oscillation, only the droplet images during the exciting period and first oscillating cycle are presented for a quick visual verification. As can be seen from the recorded current waveform, the dynamic response time of the selected power source to a step control signal is approximately 1 ms. Consequently, the exciting peak duration should be no less than 2 ms. The initial droplet lengths L_{int} in the three experiments were measured at approximately 1.2 mm.

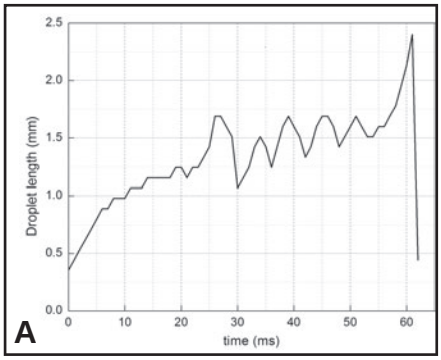

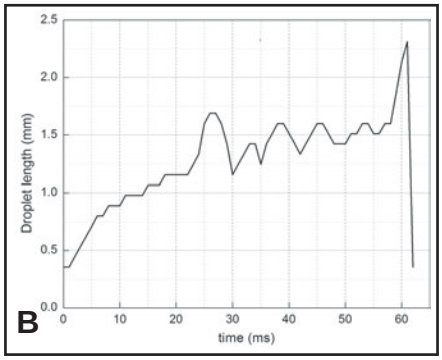

Fig. 14 — Droplet oscillation with different exciting base currents. A — I_{b2} = 10 A; B — I_{b2} = 50 A.

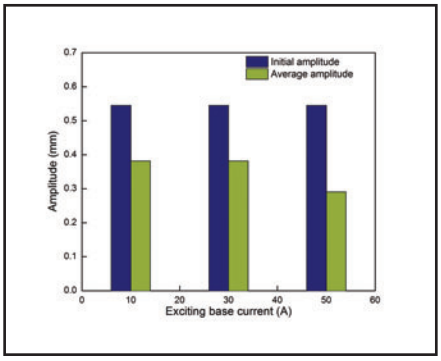

Fig. 15 — Droplet oscillation amplitude with different exciting base currents.

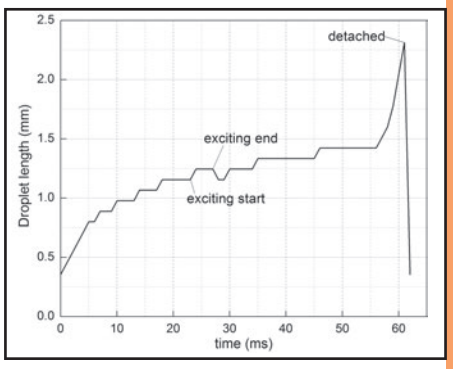

Fig. 16 — Droplet oscillation with 70-A exciting peak current.

The droplet oscillation frequencies in experiments 1–3 were all measured to be approximately 166 Hz. The oscillation periods T_{avg} were approximately 6 ms in these experiments. The equivalence of the oscillation frequency observed from these experiments is supported by the previous theoretical work that the droplet oscillation frequency is mainly determined by the droplet mass (Refs. 11, 25).

The initial droplet oscillation energy should have been believed to be mainly determined by the exciting peak current level when the droplet mass is given. This would suggest that the initial amplitude in all these three experiments should be similar as their exciting peak current and droplet mass are the same. However, this prediction is not supported by the experimental results.

Each frame 6 in Fig. 5A–C shows the elongation of the droplet at the falling edge of the exciting pulse. As aforementioned, this elongation represents the initial energy of the active oscillation. As can be seen, despite the same droplet mass and application of the same exciting current, the droplet is more elongated when applying the lower growing current. In particular, the difference among these three experiments is the exciting rising level I_R, defined as $I_e - I_g$, which is 0 A in experiment 1, but 70 and 110 A for experiments 2 and 3. The dynamic droplet length curves of the whole metal transfer cycle in experiments 1–3 are measured to demonstrate the droplet oscillations and perform a further quantitative comparison, as shown in Fig. 6A–C. It can be seen that the fluctuation of the droplet length in experiment 3 is prominently more significant, implying that its droplet oscillation energy is significantly larger than those in experiments 1 and 2.

It is now clear that the exciting peak current is not the only parameter determining the initial oscillation energy when the droplet mass is given. Instead, the initial oscillation energy is determined by the exciting raising level. In the original active oscillation method, the exciting current equals the growing current, resulting in a zero exciting raising level. The separation-based modification specifies an effective direction to increase the oscillation.

Current Waveform Optimization

Rising Level Maximization

Although the droplet oscillation can be enhanced by applying a lower growing current to enlarge the exciting rising level, the droplet growth also slows down, resulting in reduced metal transfer frequency. The current waveform should maximize the

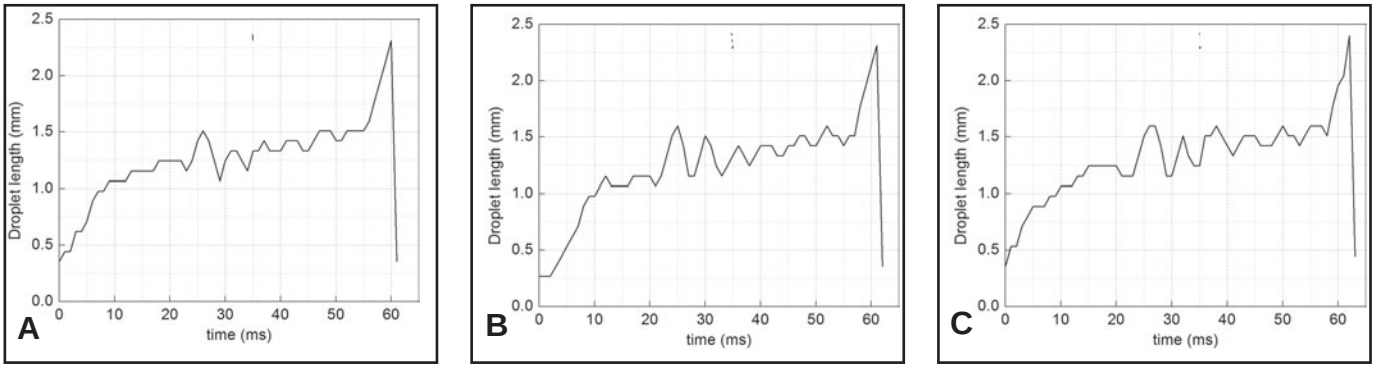

Fig. 17 — Droplet oscillation with I_e = 140 A. A — T_e = 2 ms; B — T_e= 3 ms; C — T_e = 4 ms.

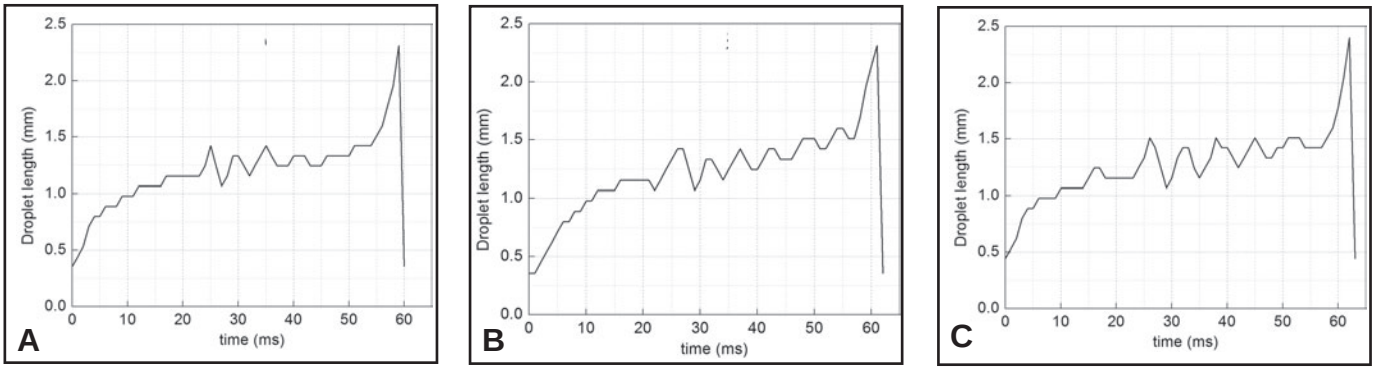

Fig. 18 — Droplet oscillation with I_e = 130 A. A — T_e = 2 ms; B — T_e = 3 ms; C — T_e = 4 ms.

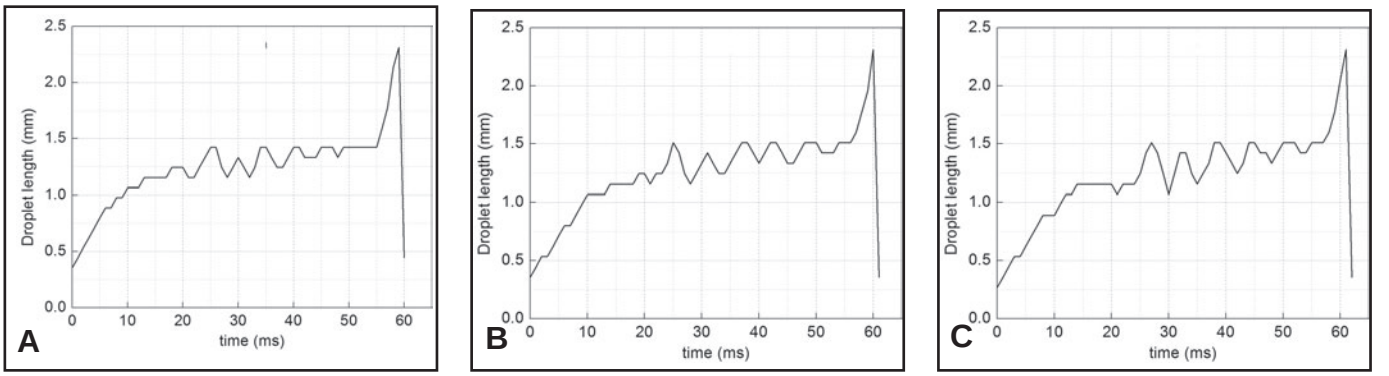

Fig. 19 — Droplet oscillation with I_e = 120 A. A — T_e = 2 ms; B — T_e = 3 ms; C — T_e = 4 ms.

rising level of the exciting pulse despite the growing current. To this end, the further optimized waveform shown in Fig. 7 is proposed. In this waveform, at the end of the growing duration, the current is first switched to the base level, and then increased to the exciting peak level. Two new parameters are introduced: the base current I_{b1} and its duration T_{b1} before exciting. The exciting rising level I_R becomes $I_e - I_{b1}$. Since the base current is approximately the lowest amperage allowed, the exciting rising level is maximized.

Preoscillation

While the intentional decrease of the current before exciting maximizes the exciting rising level to enhance the droplet oscillation, it introduces a possible need for phase match such that the base duration T_{b1} should be determined based on the growing current level. That is, when the growing current amperage is high enough, for example, 150 A, the droplet is expected to have been pre-elongated during the growing duration. As a result, when the current is changed to the first base level I_{b1}, the droplet oscillation should have been excited. This oscillation that occurs before the exciting pulse is referred to as the preoscillation in this study. In this case, the droplet downward momentum during the first base period T_{b1} can be utilized to further enhance the droplet oscillation during the second base duration T_{b2}. However, this enhancement occurs only when the exciting pulse matches the preoscillation in phase, i.e., the exciting pulse that is supposed to elongate the droplet should be applied when the droplet moves down toward the workpiece during the preoscillation. The first base duration T_{b1} should be half of the droplet oscillation period to synchronize the droplet downward motion and exciting pulse. However, if the growing current is not high enough to pre-elongate the droplet significantly, the phase match condition is not required. Hence, the first base current period in the optimized current

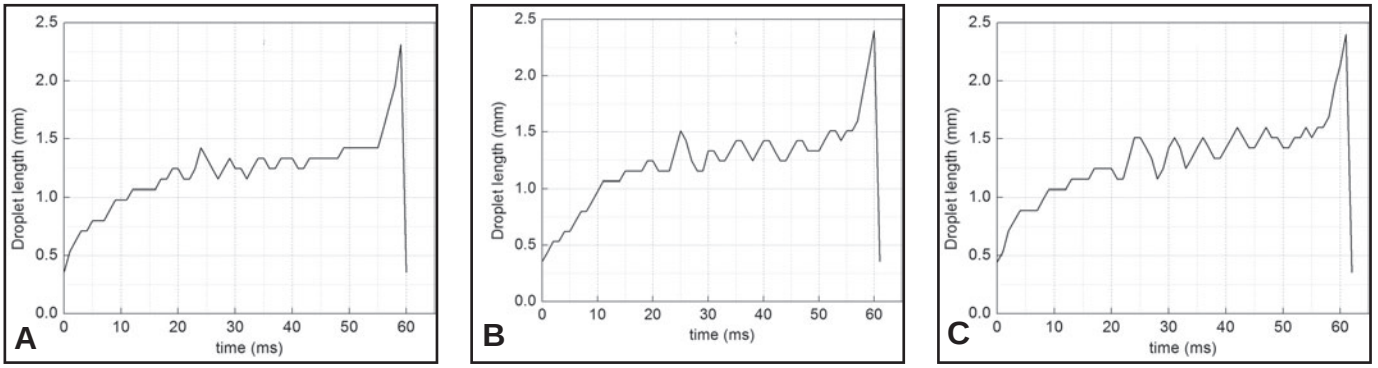

Fig. 20 — Droplet oscillation with I_e *= 110 A. A —* T_e *= 2 ms; B —* T_e *= 3 ms; C —* T_e *= 4 ms.*

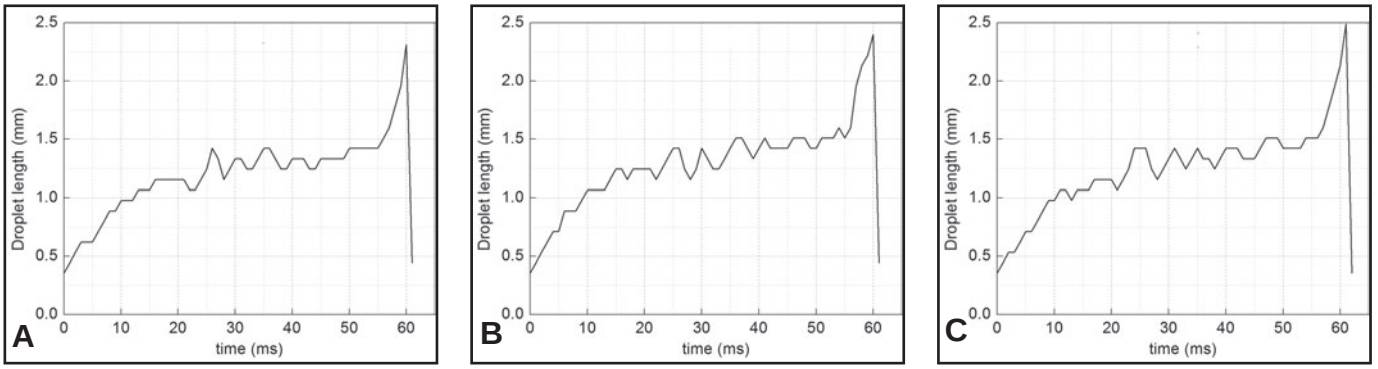

Fig. 21 — Droplet oscillation with I_e *= 100 A. A —* T_e *= 2 ms; B —* T_e *= 3 ms; C —* T_e *= 4 ms.*

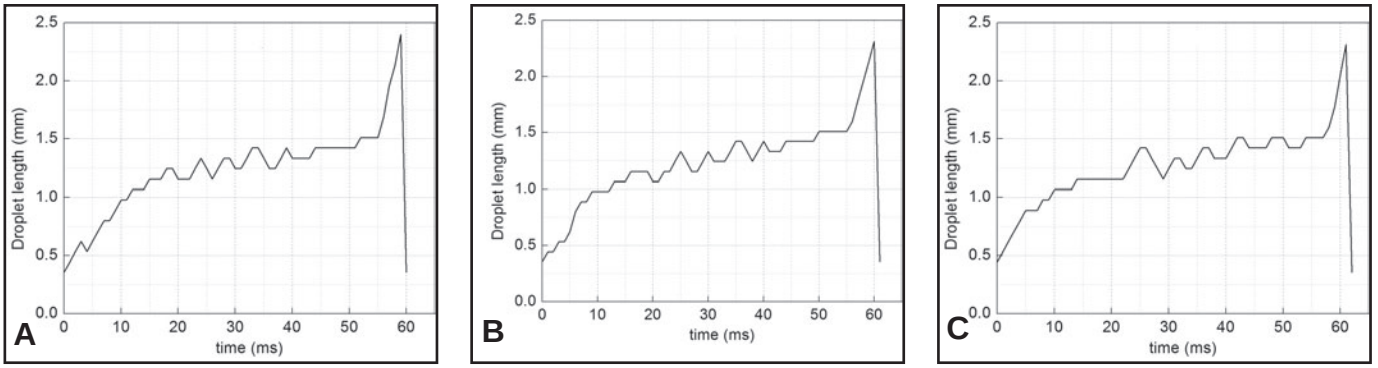

Fig. 22 — Droplet oscillation with I_e *= 90 A. A —* T_e *= 2 ms; B —* T_e *= 3 ms; C —* T_e *= 4 ms.*

waveform needs to be determined based on the growing current.

Verification of Optimization Effect

To verify the effect of the optimized waveform, which is characterized by the first base period before the exciting pulse, experiments 4 and 5 were conducted using the optimized waveform with different growing parameters listed in Table 3. The remaining waveform parameters in these two experiments were fixed: I_{b1} = 30 A, T_{b1} = 3 ms; I_e = 150 A, T_e = 4 ms; I_{b2} = 30 A, T_{b2} = 30 ms; and I_d = 165 A, T_d = 5 ms. The initial droplet mass in the two experiments were also approximately the same. To utilize the possible preoscillation to enhance the final droplet oscillation, the first base time T_{b1} was set at 3 ms to match the phase because the droplet oscillation period was approximately 6 ms for the given droplet mass in experiments 4 and 5. The recorded current waveforms and droplet oscillation images from experiments 4 and 5 are shown in Fig. 8A, B. The time interval for each frame is also 1 ms. The measured droplet length curve of experiment 4 is shown in Fig. 9.

The result from experiment 4 (using the optimized waveform for separation-based modification) is first compared with that from experiment 2 (using the simple waveform for separation-based modification). The growing and exciting parameters in the two experiments are the same. The only difference is that the exciting rising level I_R has been maximized to 120 A in experiment 4 for the exciting current and base current used while it is 70 A in experiment 2 due to the simple waveform. It can be clearly seen from corresponding frame 6 in Figs. 5B and 8A that the droplet is apparently more elongated during the exciting period in experiment 4. From Figs. 6B and 9, it also can be seen that the droplet length fluctuation in experiment 4 using the optimized waveform is much more intensive than that in experiment 2 using the simple waveform. The droplet oscillation energy in experiment 4 is sig-

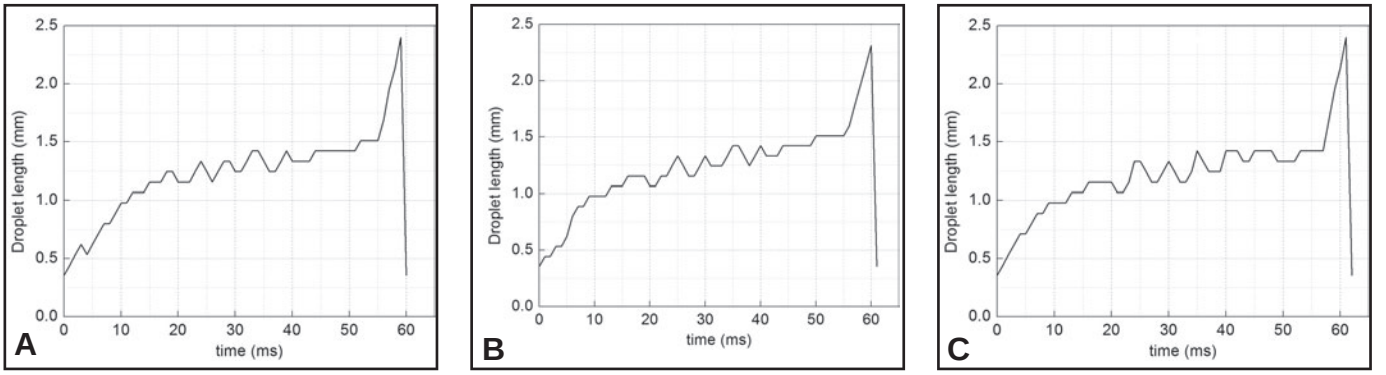

Fig. 23 — Droplet oscillation with I_e = 80 A. A — T_e = 2 ms; B — T_e = 3 ms; C — T_e = 4 ms.

Table 4 — Waveform Parameters in Experiments 6–11

No.	T_e (ms)
6	2
7	3
8	4
9	5
10	6
11	7

nificantly higher than that in experiment 2. The effect of the optimized waveform characterized by the first base period before the exciting pulse is experimentally demonstrated.

Secondly, the results of experiments 4 and 5 can be compared to demonstrate the effect of the growing current (preoscillation) on the droplet oscillation. In these two experiments, the exciting rising level I_R is 120 A in both experiments. However, the growing current is different although the droplet mass is approximately the same. In experiment 5, the growing current (150 A) is high enough to pre-elongate the droplet. In experiment 4, the growing current (80 A) is relatively low; the droplet is not significantly pre-elongated during the growing period such that the preoscillation during the first base period is quite weak. It can be seen from Fig. 8B the droplet is detached by the exciting pulse of 150 A current with only 4 ms duration due to the preoscillation in experiment 5. However, in Fig. 8A for experiment 4 where the preoscillation is insignificant, the droplet is not detached. The oscillation in experiment 5 (with preoscillation) is stronger. The effect of the preoscillation in enhancing the oscillation is demonstrated, and it is apparently an additional advantage of the optimized waveform.

To further perform a global quantitative analysis of the current waveform (original, simple, and optimized) effect on the droplet oscillation, the initial amplitude A_{int} and average amplitude A_{avg} for experiments 1–4 are measured and calculated. The results are shown in Fig. 10.

In addition, the following can be seen:

1. For experiments 1–3, in which the simple current waveform was used, the exciting rising level is 0, 70, and 110 A, respectively. From Fig. 10, the droplet oscillation amplitude increases with the increased exciting rising level. The average amplitude in experiment 2 is 42.8% higher than that in experiment 1, and the average amplitude in experiment 3 is, respectively, 171 and 90% higher than that in experiments 1 and 2. Much stronger droplet oscillation is achieved by using the simple waveform for separation-based modification with a reduced growing current when the exiting current is given.

2. In comparison with experiment 3, the magnitude of the droplet oscillation in experiment 4 is improved. As can be seen from Fig. 10, the initial amplitude of experiment 4 is 25% higher than that in experiment 3, and the average amplitude is increased by 7.9%. This improvement is achieved because the exciting rising level I_R is 9.09% higher than that in experiment 3. This increase in the exciting rising level I_R is the result of the first base period that characterizes the optimized waveform, which decouples the exciting rising level I_R from the growing current. The growing current can be freely selected to grow the droplet and control the metal transfer frequency. It is apparent that the optimized waveform is responsible for the improvement.

In summary, it has been found that a larger exciting rising level produces a stronger droplet oscillation. The optimized waveform proposed provides a method to maximize the exciting rising level by adding a base period before the exciting pulse. This addition of additional base period also introduces a possible preoscillation, and this preoscillation may further enhance the oscillation if the duration of the added base period facilitates a phase match with the exciting pulse.

Optimization of Waveform Parameters

Although the optimized waveform provides a method to maximize the exciting rising level, there are still other parameters which specify the actual waveform and can be optimized to maximize the oscillation. These parameters include the exciting peak duration, exciting peak/base current, and growing duration. A series of experiments was designed and conducted in this section to analyze the effects on the droplet oscillation and determine the optimal selection of these parameters.

Exciting Peak Duration

In this subsection, the exciting peak duration T_e was set into several different levels to analyze its influence on the droplet oscillation. If the exciting peak duration is too long, the droplet may grow to a relatively large size and then get detached by the gravity such that the desired droplet oscillation cannot be observed. On the other hand, if the peak duration is too narrow, the droplet probably could not be elongated enough, and the droplet oscillation would be too weak to be observed. In this sense, an appropriate range for the exciting peak duration is needed. Based on the results from experiments 3 and 4, it has been confirmed that the droplet oscillation is reasonably strong by using 4 ms exciting peak duration. Furthermore, the droplet oscillations with other different exciting peak duration levels also need to be studied to lead a deeper comprehension on the droplet oscillation behavior. Hence, experiments 6–11 were conducted in which the exciting peak duration T_e was the only varying variable. As can be seen from Table 4, the exciting peak duration was changed from 2 to 7 ms in experiments 6–11. The other waveform parameters in this group of experiments were fixed: I_g = 80 A, T_g = 20 ms; I_{b1} = 30 A, T_{b1} = 3 ms; I_e = 150 A; I_{b2} = 30 A, T_{b2} = 30 ms; and

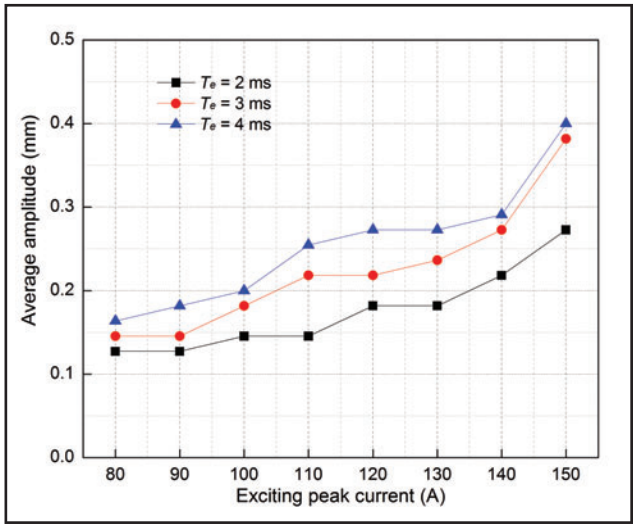

Fig. 24 — Average amplitude with different exciting peak currents.

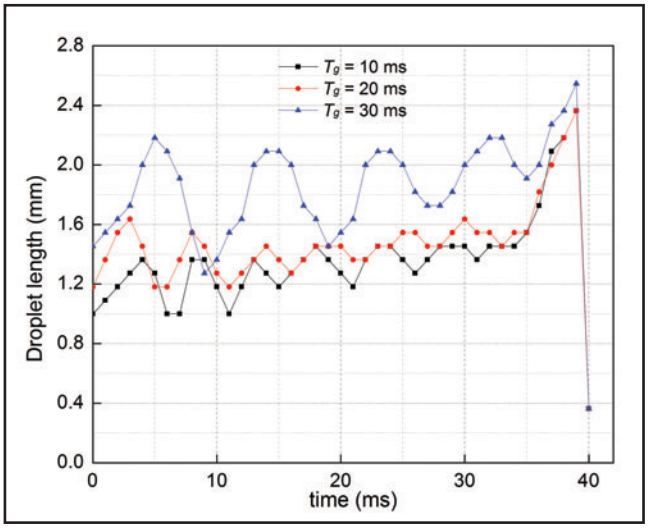

Fig. 25 — Droplet oscillation with different growing durations.

I_d = 165 A, T_d = 5 ms.

The dynamic droplet length curves are measured, as shown in Fig. 11A–F, for experiments 6–11, respectively. The initial amplitude A_{int} and average amplitude A_{avg} in this group of experiments are also measured to demonstrate how the exciting peak duration influences the droplet oscillation magnitude, as shown in Fig. 12.

As can be seen from Fig. 11A–C, the droplet length keeps increasing during the whole exciting peak period when the exciting peak duration is 2–4 ms. When the exciting peak duration is 5–7 ms, as shown in Fig. 11D–F, the droplet is elongated to its maximum displacement in approximately 3 ms from the start of the exciting pulse. In the rest of the exciting peak period, the droplet length is no longer increased and even slightly reduced. The fluctuations of the droplet length curve with the exciting duration of 3 and 4 ms are approximately in the same level. The fluctuation in experiment 6 with the exciting duration of 2 ms is significantly weaker. This result agrees with the logical prediction that weaker droplet oscillation is associated with shorter exciting duration. However, the unexpected result is that the droplet oscillation also got weaker when the exciting peak duration exceeded 4 ms. As can be seen from Fig. 11C–F, the fluctuation of the droplet length gets weaker with the increased exciting peak duration (from 4 to 7 ms). As can be calculated from Fig. 12, the average amplitude of the droplet oscillation with 5 ms exciting peak duration is approximately 36.6% lower than that with 4 ms exciting peak duration, even 13.3% lower than that with 2 ms exciting duration.

Take experiment 11 using 7 ms exciting peak duration as an example to analyze the dynamic motion of the droplet during the entire exciting peak period, as shown in Fig. 13, with the time interval for each image being 0.4 ms. During the period as frames 1–8 show (3.2 ms), the droplet length keeps increasing until it reaches the maximum displacement, and the arc length is stable. After that, the droplet length stops increasing, while the droplet starts to move upward and the arc length is slightly increased by 0.6 mm, as shown in frames 9–16 of Fig. 13. Such a fluctuation level of the arc length is absolutely acceptable in the GMAW process. It can be seen that the droplet is getting slightly less elongated during its upward moving period.

A qualitative analysis of this phenomenon is performed based on the dynamic force balance model (DFBM) of metal transfer (Ref. 11), in which droplet momentum is considered. The droplet momentum contributes to attaching or detaching the droplet, depending on the droplet moving directions. During the exciting peak period, the wire melting rate is significantly increased because the current is increased. Meanwhile, the wire feed speed can be considered constant during this several-millisecond short period, because the adjustment on the wire feed speed is much slower. As a result, the wire melting rate exceeds the wire feed speed during the exciting peak period. The wire is burned back toward the contact tip, and the droplet moves upward.

It is the upward momentum of the droplet that partly counteracts the electromagnetic force. Therefore, the droplet gets less elongated, and the droplet oscillation is weakened.

The dynamic motion of the droplet during the whole exciting peak period clearly reveals two effects of the current increase (from the base level to exciting peak level) on the droplet:

1. Force Effect. The high electromagnetic force generated by the exciting peak current drags the droplet into an elongated shape. Based on the experimental results, we can see that this effect takes place instantly once the current is switched to the exciting peak level.

2. Thermal Effect. Because the current is increased, the wire melting rate increases to exceed the wire feed speed. The wire is burned back slightly, in other words, the arc length increases slightly, and the droplet moves upward to the wire tip during the dynamic process. The upward momentum is produced, and it weakens the droplet oscillation. However, the so-called thermal effect demonstrates a slight delay to the current increase, which is approximately 3 ms measured from the experimental results.

In summary, it is the upward momentum of the droplet during the exciting period that weakens the droplet oscillation, but the delay of its occurrence to the current increase determines that there is a threshold of exciting peak duration for the droplet oscillation to get weaker. Based on the results as Figs. 11 and 12 show, the threshold level is 4 ms, and the optimal selection of the exciting peak duration is confirmed to be 3 to 4 ms. An exciting peak duration of 2 ms is also acceptable. However, the exciting peak duration exceeding 4 ms is not recommended.

Exciting Base Current

As mentioned above, the droplet oscillation is a damping process. When the exciting peak current is switched to the base level, the electromagnetic force is reduced but not eliminated, and it contributes to decay of the droplet oscillation. In this sense, an applicable exciting base current

Table 5 — Exciting Parameters of Experiments 14–34

No.	I_e(A)	T_e (ms)
14	140	2
15	140	3
16	140	4
17	130	2
18	130	3
19	130	4
20	120	2
21	120	3
22	120	4
23	110	2
24	110	3
25	110	4
26	100	2
27	100	3
28	100	4
29	90	2
30	90	3
31	90	4
32	80	2
33	80	3
34	80	4

should be determined. The criteria should be that the droplet oscillation will not decay too fast to weaken the beneficial downward momentum significantly and that the arc would still burn stably. To this end, the exciting base current I_{b2} is set to be 10 and 50 A in experiments 12 and 13, respectively, to verify its effect on the droplet oscillation. The other current waveform parameters in the two experiments were fixed to be I_g = 80 A, T_g = 20 ms; I_{b1} = 30 A, T_{b1} = 3 ms; I_e = 150 A, T_e = 4 ms; T_{b2} = 30 ms; and I_d = 165 A, T_d = 5 ms. The result of experiment 8 is referred to as a comparison, in which the exciting base current I_{b2} is 30 A, and the other parameters are the same with those in experiments 12 and 13.

The measured droplet oscillation from experiments 12 and 13 are shown in Fig. 14A and B, respectively. It can be seen that the fluctuation of droplet length in experiment 13 is weaker than that in experiment 12. The initial amplitude A_{int} and average amplitude A_{avg} in experiments 8, 12, and 13 are calculated correspondingly, as shown in Fig. 15. It can be seen that the initial amplitudes in the three experiments are quite similar, because the same growing and exciting parameters were used in the three experiments. However, the average amplitude demonstrates a down trend with the increased exciting base current. As shown in Fig. 15, the average amplitude with the base current of 10 and 30 A are measured being similar, but that with the exciting base current of 50 A is approximately 24% weaker. Furthermore, with respect to the fact that the arc burning at 30 A is more stable than that burning at 10 A, the exciting base current was fixed at 30 A in the following experiments as an optimal selection.

Table 6 — Growing Duration of Experiments 35–37

No.	T_g (ms)
35	10
36	20
37	40

Exciting Peak Current

The droplet oscillation behavior is further analyzed by changing the exciting peak current in this subsection. The exciting peak current certainly cannot be higher than the transition current. However, it is also doubtless that the exciting peak current cannot be lower than a specific level. Otherwise, the droplet will not be elongated and then oscillated effectively. This minimum exciting peak current level is defined as the oscillating transition current in this paper. Based on the study above, the selections of the current waveform and exciting peak duration are optimized. An exciting peak current, I_e of 150 A, is used to elongate the droplet according to the transition current of 165 A. The optimal range of the exciting peak duration is also confirmed to be 2–4 ms. In this subsection, the oscillating transition current is first verified by experiments, then a group of experiments with a different combination of exciting peak current I_e and duration T_e are conducted. The droplet oscillations are recorded and analyzed.

The oscillating transition current was tested to be 70 A by the experiments in which the exciting peak current is stepping down, while the exciting peak duration T_e was fixed at 4 ms. The droplet length curve with the exciting peak current of 70 A is shown in Fig. 16. It can be seen from the figure that the droplet is almost not oscillated at all. Based on this result, the selected exciting peak current I_e changes from 140 to 80 A, stepped down by 10 A each time, as shown in Table 5; plus, the exciting peak duration ranges from 2 to 4 ms for each selected exciting peak current level. The other waveform parameters are fixed to be the same: I_g = 80 A, T_g = 20 ms; I_{b1} = 30 A, T_{b1} = 3 ms; I_{b2} = 30 A, T_{b2} = 30 ms; and I_d = 165 A, T_d = 5 ms.

The droplet length was measured to demonstrate the dynamic droplet oscillation in experiments 14–34, as shown in Figs. 17 to 23, respectively. The average amplitude A_{avg} was also calculated to quantitatively reveal the relationship between the droplet oscillation energy and exciting current, which is shown in Fig. 24. It can be seen that the average amplitude of the droplet oscillation presents a parabolic growth approximately with the increased exciting peak current. As calculated before, the average amplitude of the droplet oscillation in experiment 1, applying the original waveform and 150 A exciting peak current, is approximately 0.124 mm. By comparing this result with those in experiments 32–34, it is found that the same or even stronger droplet oscillation is achieved with only 80 A exciting peak current by applying the optimized current waveform. In this sense, the enhancement of the optimized current waveform on the droplet oscillation is further ensured. Meanwhile, the average current is 79.5 A in experiment 1, but only approximately 58 A in experiment 32 and 60 A in experiment 34. The heat input is significantly reduced by applying the optimized current waveform.

Growing Duration

As introduced previously, the initial droplet size/mass can be controlled by adjusting the growing duration. In this subsection, the growing duration T_g is set at three different levels, and the remaining waveform parameters are fixed: I_g = 80 A; I_{b1} = 30 A, T_{b1} = 3 ms; I_e = 140 A, T_e = 3 ms; I_{b2} = 30 A, T_{b2} = 30 ms; and I_d = 165 A, T_d = 5 ms. As shown in Table 6, the growing duration is double increased from 10 to 40 ms in experiments 35 to 37, so the initial droplet mass is also approximately doubled. The droplet oscillations in these three experiments were measured and shown in Fig. 25. It demonstrates that the initial droplet size is 0.98, 1.16, and 1.42 mm for experiment 35–37, respectively. The droplet oscillation frequencies were measured to be 216, 183, and 133 Hz, respectively. This result agrees with the theoretical calculation result that the droplet oscillation frequency changes along with the droplet mass (Refs. 11, 25).

Conclusions and Future Work

The dynamic droplet oscillation behavior was systematically studied in this work. Stronger droplet oscillation and lower heat input were achieved by applying the optimized current waveform. The effects of the waveform parameters on the excited droplet oscillation were revealed by a number of experiments. The optimal range of current waveform parameters was determined.

1. The current waveform applied to excite the droplet oscillation is modified. The critical modification is that the droplet growing and exciting periods are separated. It is found that the droplet oscillation can be significantly enhanced by

enlarging the exciting rising level. The average current is meanwhile reduced. Based on this result, the modified current waveform is further optimized to obtain maximized droplet oscillation energy with any level of growing current.

2. The influence of the exciting parameters on the droplet oscillation was analyzed. It was found that the exciting peak duration is a key parameter determining the droplet oscillation. Its optimal range was confirmed in experiments to be 3–4 ms while 2 ms is also acceptable. The droplet oscillation with a different exciting base current and peak current was also studied. The optimal base current is considered to be 30 A according to the experimental results. The exciting transition current was defined and tested to be 70 A. The droplet oscillations using the exciting peak current ranged in 80–140 A were measured. The results demonstrate that the droplet oscillation energy increased approximately in a parabolical way when the exciting peak current was stepping up.

3. The growing duration was set in a group of values to verify its influence on the droplet oscillation. It is demonstrated that the droplet oscillation frequency changes significantly with the growing duration. The droplet mass gets larger with increased growing duration, so the droplet frequency is decreased.

As future work, the correlation of the droplet oscillation with the arc voltage needs to be analyzed such that the droplet motion can be monitored by sensing the arc voltage signal. Furthermore, a closed-loop control of the phase match based on the feedback of arc voltage is expected to maximize the enhancement on metal transfer during the droplet oscillation. Based on this work, the minimum detaching current utilizing the active droplet oscillation will be tested with a different combination of the exciting peak current (80–150 A) and duration (2–4 ms). In addition, such closed-loop controlled active droplet oscillation technology may be further applied into the laser-enhanced GMAW process to reduce the required laser power.

Acknowledgments

This work is supported by the State Key Laboratory of Advanced Welding and Joining, Harbin Institute of Technology, Harbin, China, and the National Science Foundation under grant CMMI-0825956. Jun Xiao greatly appreciates the scholarship from the China Scholarship Council that funds his visit to the University of Kentucky.

References

1. Sadler, H. 1999. A look at the fundamentals of gas metal arc welding. *Welding Journal* 78(5): 45–50.

2. *The Procedure Handbook of Arc Welding*. 1994. The Lincoln Electric Co., Cleveland, Ohio. ISBN 99949-25-2-2.

3. O'Brien, R. L. 1991. *Welding Handbook*. Vol. 2: Welding Processes. 8th edition, American Welding Society, Miami, Fla.

4. Stava, E. K. 1993. A new, low-spatter arc welding machine. *Welding Journal* 72(1): 25–29.

5. Stava, E. K. 1992. System and method of short circuiting arc welding. U.S. Patent #5,148,001.

6. Himmelbauer, K. 2005. The CMT-Process — A revolution in welding technology. IIW Doc XII-1875-05, 20-27.

7. Kim, Y.-S., and Eagar, T. W. 1993. Analysis of metal transfer in gas metal arc welding. *Welding Journal* 72(6): 269-s to 278-s.

8. Lancaster, J. F. 1984. *The Physics of Welding*. Pergamon Press, Oxford, England.

9. Iszink, J. H., and Piena, M. J. 1986. Experimental investigation of drop detachment and drop velocity in GMAW. *Welding Journal* 65(11): 289-s to 298-s.

10. Essers, W. G., and Walter, R. 1981. Heat transfer and penetration mechanisms with GMA and plasma-GMA welding. *Welding Journal* 60(2): 37-s to 42-s.

11. Choi, J. H., Lee, J., and Yoo, C. D. 2001. Dynamic force balance model for metal transfer analysis in arc welding. *Journal of Physics D: Applied Physics* 34: 2658–2664.

12. Shi, Y., Liu, X., Zhang, Y. M., and Johnson, M. 2008. Analysis of metal transfer and correlated influences in dual-bypass GMAW of aluminum. *Welding Journal* 87(9): 229-s to 236-s.

13. Li, K., and Zhang, Y. M. 2007. Metal transfer in double-electrode gas metal arc welding. *Journal of Manufacturing Science and Engineering — Transactions of the ASME* 129(6): 991–999.

14. Thomsen, J. S. 2006. Control of pulsed gas metal arc welding. *International Journal of Modelling, Identification, and Control* 1(2): 115–125.

15. Zheng, B., and Kovacevic, R. 2001. A novel control approach for the droplet detachment in rapid prototyping by 3D welding. *Journal of Manufacturing Science and Engineering* 123: 348–355.

16. Wu, Y., and Kovacevic, R. 2002. Mechanically assisted droplet transfer process in gas metal arc welding. *Journal of Engineering Manufacturing* 216: 555–564.

17. Yang, S. Y. 1998. Projected droplet transfer control with additional mechanical forces (AMF) in MIG/MAG welding process. PhD dissertation, Harbin Institute of Technology.

18. Allum, C. J. 1985. Welding technology data: pulsed MIG welding. *Welding and Metal Fabrication* 53: 24–30.

19. Kim, Y. S., and Eagar, T. W. 1993. Metal transfer in pulsed current gas metal arc welding. *Welding Journal* 72(7): 279-s to 287-s.

20. Amin, M. 1983. Pulse current parameters for arc stability and controlled metal transfer in arc welding. *Metal Construction* 15: 272–278.

21. Zhang, Y. M., Liguo, E., and Kovacevic, R. 1998. Active metal transfer control by monitoring excited droplet oscillation. *Welding Journal* 77(9): 388-s to 395-s.

22. Zhang, Y. M., and Liguo, E. 1999. Method and system for gas metal arc welding. U.S. Patent #6,008,470.

23. Wang, G., Huang, P. G., and Zhang, Y. M. 2004. Numerical analysis of metal transfer in gas metal arc welding under modified pulsed current conditions. *Metallurgical and Materials Transactions B* 35(5): 857–866.

24. Zhang, Y. M., and Li, P. J. 2001. Modified active control of metal transfer and pulsed GMAW of titanium. *Welding Journal* 80(2): 54-s to 61-s.

25. Li, S. K. 2004. Numerical analysis of droplet transfer in active control mode of the pulsed GMAW. Master's dissertation. Shandong University.

26. Huang, Y., and Zhang, Y. M. 2010. Laser-enhanced GMAW. *Welding Journal* 89(9): 181-s to 188-s.

27. Huang, Y., and Zhang, Y. M. 2011. Laser-enhanced metal transfer — Part 1: System and observations. *Welding Journal* 90(10): 183-s to 190-s.

28. Huang, Y., and Zhang, Y. M. 2011. Laser-enhanced metal transfer — Part 2: Analysis and influence factors. *Welding Journal* 90(11): 206-s to 210-s.